# C1.3 Laminar Boundary Layer on a Flat Plate

Lei Shi and Z.J. Wang

University of Kansas

## I. Code Description

HpMusic (HP adaptive MUltiphysics SImulation Code) is an adaptive high-order correction procedure via reconstruction (CPR) solver. It can support up to $6^{th}$ order CPR schemes on hybrid QUAD/TRI meshes in 2D and HEX meshes in 3D. The code is parallelized using domain partitioning and MPI message passing library. An adjoint-based HP-adaptation is available to control the discretization error and estimate the output error.

## II. Case Summary

All simulations start from the free stream. A GMRES implicit time solver with ILU preconditioning is used for the time integration. The $L_2$ norm of the x-momentum residual is utilized to monitor the convergence. The initial residual is dropped by 10 orders of magnitude for all cases in this test. The CPU time is expressed in work units, which includes the time taken for the primal solve, the adjoint solve and the error estimation. The simulations were performed in the serial mode. TauBench ran in 9.65s.

## III. Results

### III.A. Reference Output

The reference drag coefficient is obtained using the adjoint-based h-adaptation. We use the $4^{th}$ order CPR scheme with the Gauss points as the solution points and the flux points. The DG correction function and the LP approach is used for all runs. The ref0 grid from the workshop website is used as the initial mesh for the adaptations, which consists of 140 elements. Isotropic and anisotropic h-adaption driven by the drag adjoint are performed. For anisotropic adaptation, the local output error sampling procedures is used to find the optimal refinement option for each candidate element. Figure III.3 shows the initial mesh and the adapted meshes. Mach contours are displayed in Figure III.1. The leading point and the elements around the lower boundary are refined repeatedly on each adaptation level. And both of the anisotropic and isotropic adaptation try to refine the leading point isotropically.

The convergence histories of the drag coefficients are shown in Figure III.2. On the final adaptation stage, the estimated output error is around $7e^{-10}$, which has around $2e^5$ number of degrees of freedom. The truth $C_D$ are chosen from the final adaptation stage as

$$C_D = 0.0013116860 \pm 7e^{-10}$$

### III.B. Results

Isotropic and anisotropic h-adaption driven by drag adjoint are tested. Uniform h-refinement is performed to compare those adaptation strategies. The CPR method with the Gauss points as the SPs/FPs and the LP approach is used in the discretization. Below figures and tables show the requested results for this case. Adaptations with $p = 1$ start from ref2 quadrilateral mesh provided by the workshop website, which has

2240 elements. Adaptations with $p = 2$ start from the ref1 quadrilateral mesh , which has 560 elements. And adaptations with $p = 3$ and $p = 4$ start from the ref0 quadrilateral mesh , which has 140 elements.

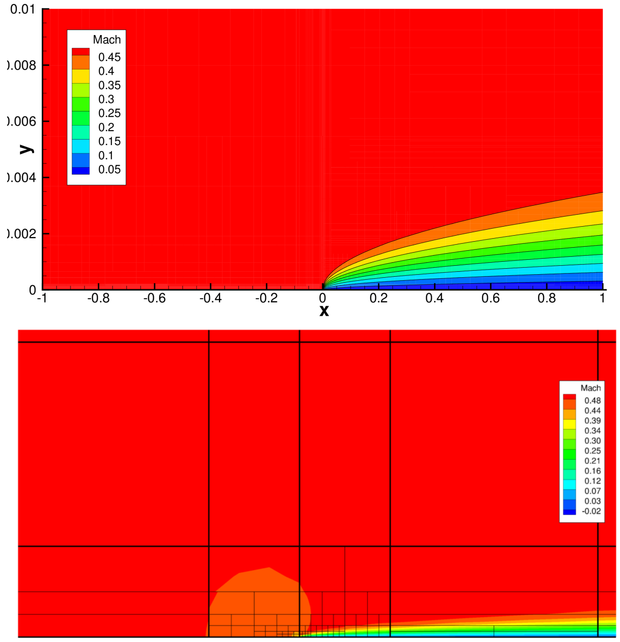


Figure III.1: Mach number contours for the laminar flat plate problem on the adapted mesh at $M_0 = 0.5$, $Re = 10^6$.

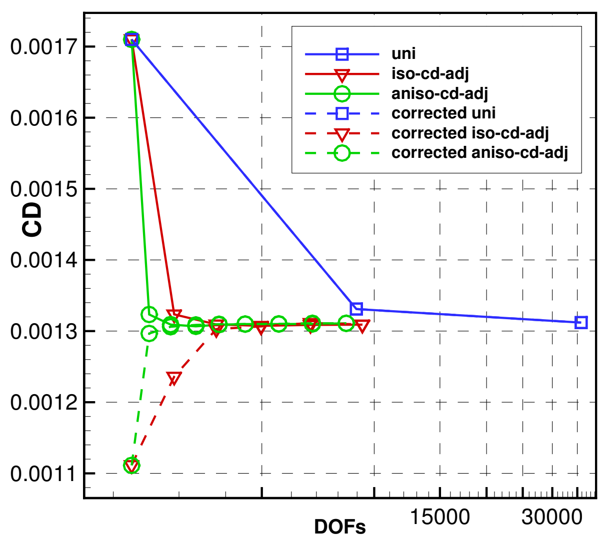


Figure III.2: CD convergence for the laminar flat plate problem at $M_0 = 0.5$, $Re = 10^6$ ($p = 3$).

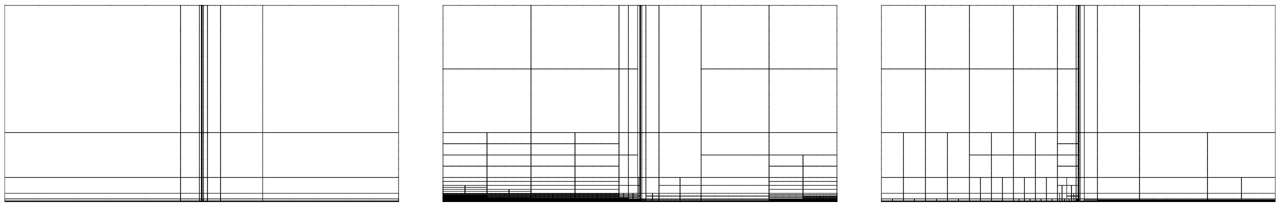

(a) The initial mesh (b) Isotropic adapted mesh (c) Anisotropic adapted mesh

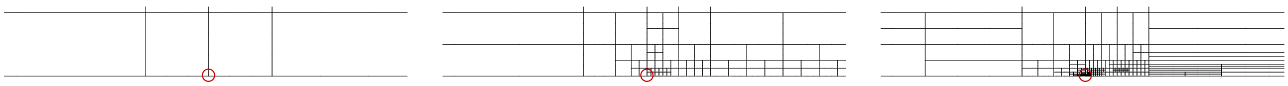

(d) Zoom in, initial mesh (e) Zoom in, isotropic adapted mesh (f) Zoom in, anisotropic adapted mesh

Figure III.3: Isotropic and anisotropic adapted mesh for the laminar flat plate problem at $M_0 = 0.5$, $Re = 10^6$. Red circle indicates the leading point ($k = 3$).

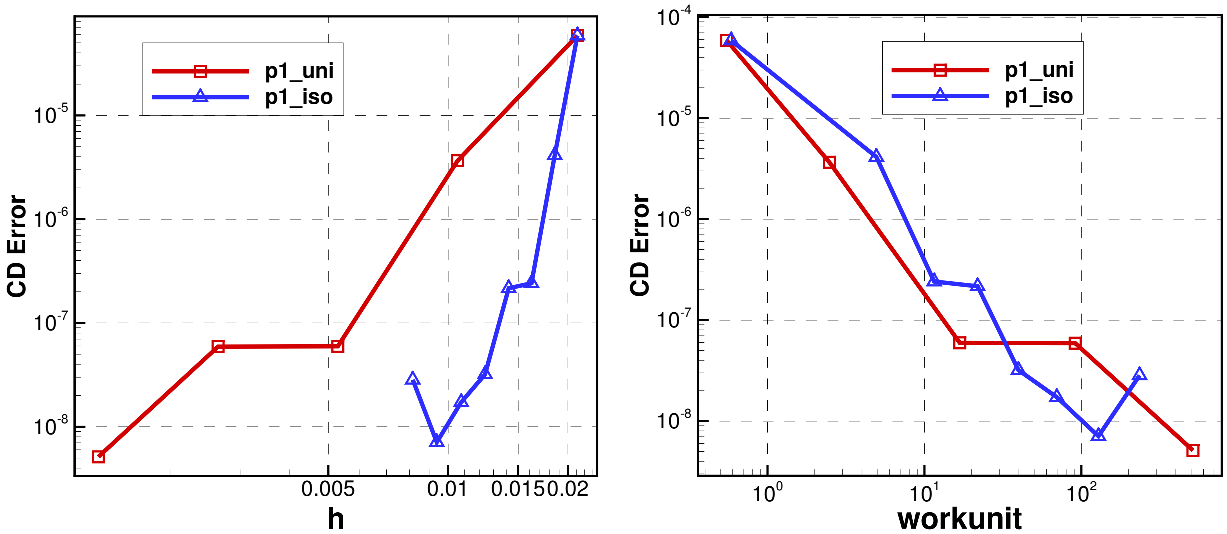


(a) p1

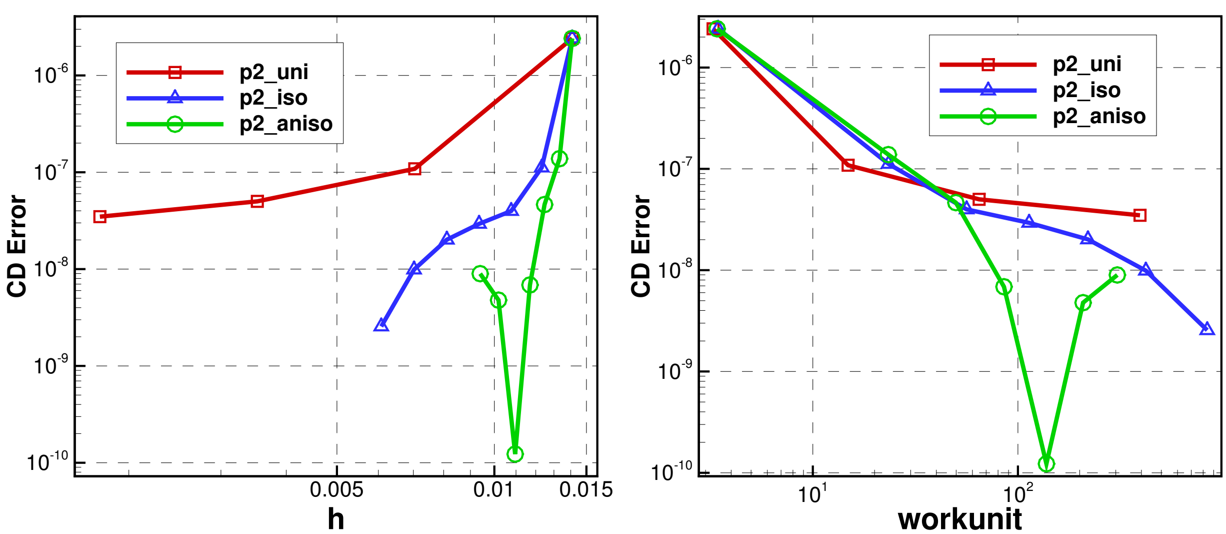


(b) p2

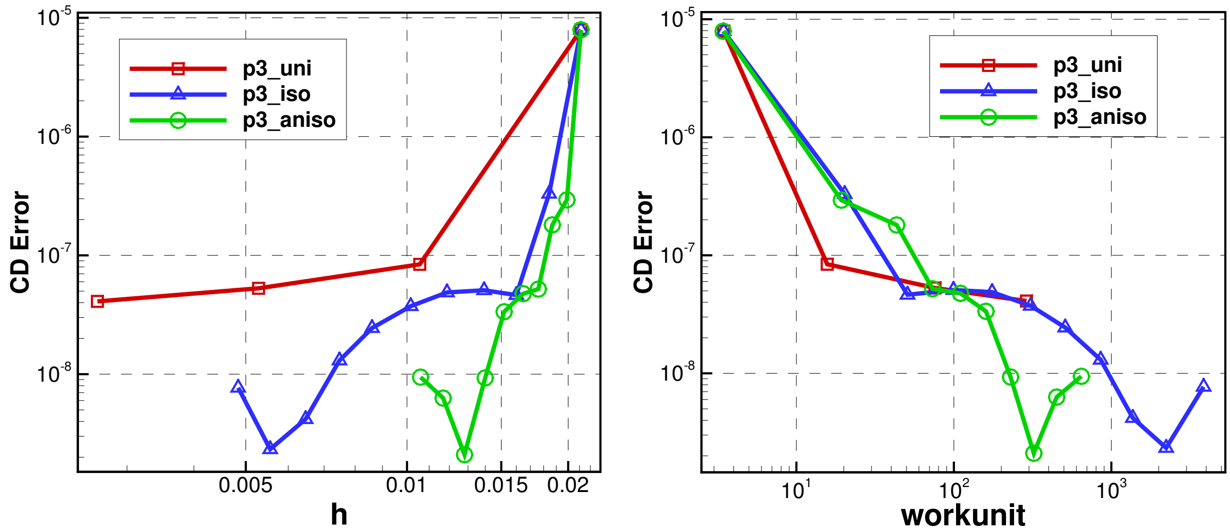


(c) p3

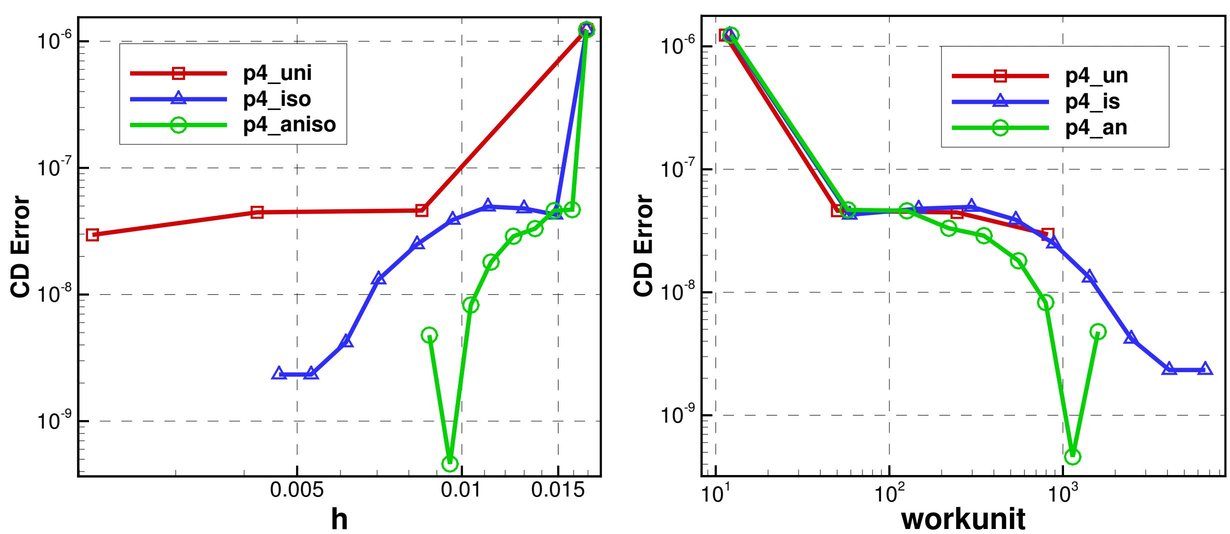


(d) p4

Figure III.2: Drag coefficient error along with the lengths and the work units.

Table 1: Isotropic adaptation using drag adjoint $p = 1$.

| adaptation stages | cell | h | $C_D$ | $C_D$ error | work units |
|---|---|---|---|---|---|
| 1 | 560 | 2.113E-02 | 1.2528363150E-03 | 5.885E-05 | 5.865E-01 |
| 2 | 728 | 1.853E-02 | 1.3075531460E-03 | 4.133E-06 | 4.937E+00 |
| 3 | 953 | 1.620E-02 | 1.3114447938E-03 | 2.412E-07 | 1.154E+01 |
| 4 | 1,240 | 1.420E-02 | 1.3114697067E-03 | 2.163E-07 | 2.183E+01 |
| 5 | 1,631 | 1.238E-02 | 1.3116539922E-03 | 3.201E-08 | 3.972E+01 |
| 6 | 2,150 | 1.078E-02 | 1.3117032358E-03 | 1.724E-08 | 6.978E+01 |
| 7 | 2,851 | 9.364E-03 | 1.3116789050E-03 | 7.095E-09 | 1.284E+02 |
| 8 | 3,766 | 8.148E-03 | 1.3117144117E-03 | 2.841E-08 | 2.349E+02 |

Table 2: Anisotropic adaptation using drag adjoint $p = 2$.

| adaptation stages | cell | h | $C_D$ | $C_D$ error | work units |
|---|---|---|---|---|---|
| 1 | 560 | 1.409E-02 | 1.3092741137E-03 | 2.412E-06 | 3.415E+00 |
| 2 | 626 | 1.332E-02 | 1.3115478214E-03 | 1.382E-07 | 2.335E+01 |
| 3 | 714 | 1.247E-02 | 1.3116395567E-03 | 4.644E-08 | 4.981E+01 |
| 4 | 812 | 1.170E-02 | 1.3116791379E-03 | 6.862E-09 | 8.550E+01 |
| 5 | 925 | 1.096E-02 | 1.3116861228E-03 | 1.228E-10 | 1.377E+02 |
| 6 | 1,071 | 1.019E-02 | 1.3116907794E-03 | 4.779E-09 | 2.078E+02 |
| 7 | 1,259 | 9.394E-03 | 1.3116949704E-03 | 8.970E-09 | 3.051E+02 |

Table 3: Anisotropic adaptation using drag adjoint $p = 3$.

| adaptation stages | cell | h | $C_D$ | $C_D$ error | work units |
|---|---|---|---|---|---|
| 1 | 140 | 2.113E-02 | 1.3037686003E-03 | 7.917E-06 | 3.429E+00 |
| 2 | 158 | 1.989E-02 | 1.3113927562E-03 | 2.932E-07 | 1.931E+01 |
| 3 | 179 | 1.869E-02 | 1.3118666830E-03 | 1.807E-07 | 4.335E+01 |
| 4 | 202 | 1.759E-02 | 1.3116339687E-03 | 5.203E-08 | 7.326E+01 |
| 5 | 230 | 1.648E-02 | 1.3116383925E-03 | 4.761E-08 | 1.102E+02 |
| 6 | 271 | 1.519E-02 | 1.3116524788E-03 | 3.352E-08 | 1.599E+02 |
| 7 | 319 | 1.400E-02 | 1.3116766931E-03 | 9.307E-09 | 2.291E+02 |
| 8 | 381 | 1.281E-02 | 1.3116881019E-03 | 2.102E-09 | 3.218E+02 |
| 9 | 458 | 1.168E-02 | 1.3116922928E-03 | 6.293E-09 | 4.499E+02 |
| 10 | 556 | 1.060E-02 | 1.3116954360E-03 | 9.436E-09 | 6.450E+02 |

Table 4: Anisotropic adaptation using drag adjoint $p = 4$.

| adaptation stages | cell | h | $C_D$ | $C_D$ error | work units |
|---|---|---|---|---|---|
| 1 | 140 | 1.690E-02 | 1.3104532845E-03 | 1.233E-06 | 1.222E+01 |
| 2 | 158 | 1.591E-02 | 1.3116392074E-03 | 4.679E-08 | 5.768E+01 |
| 3 | 184 | 1.474E-02 | 1.3116400223E-03 | 4.598E-08 | 1.263E+02 |
| 4 | 216 | 1.361E-02 | 1.3116528280E-03 | 3.317E-08 | 2.198E+02 |
| 5 | 259 | 1.243E-02 | 1.3116571354E-03 | 2.886E-08 | 3.504E+02 |
| 6 | 313 | 1.130E-02 | 1.3116679620E-03 | 1.804E-08 | 5.548E+02 |
| 7 | 371 | 1.038E-02 | 1.3116777409E-03 | 8.259E-09 | 7.954E+02 |
| 8 | 442 | 9.513E-03 | 1.3116855407E-03 | 4.593E-10 | 1.138E+03 |
| 9 | 526 | 8.720E-03 | 1.3116907794E-03 | 4.779E-09 | 1.595E+03 |